SFPE Europe Magazine

4th Quarter - 2025

<u>A word from the Editor</u>

All,

It has finally arrived—the last issue of the year. It is a bit later than usual, but as good as ever.

First of all, I would like to express my gratitude to the Editorial Team, who continue to identify and source articles for us. Keeping up with deadlines is always a challenge, but in the end, we manage to complete each issue and deliver it to you.

In this issue, we have four excellent articles for you to read: three technical articles and one highlighting chapter news. I would like to emphasize that we are always happy to receive information from your chapter events. By doing so, we aim to strengthen relationships between chapters and also demonstrate that our work is not only about technical parameters and emerging technologies.

Each year, we maintain a steady publication rate of more than 20 articles. Our future goal is to see whether this number can be increased slightly.

This time of year is always very busy for everyone, with projects being finalized and preparations underway for the Christmas holidays. That said, I truly hope you will find some time to read at least a few of the articles in this final issue of the year.

I would also like to highlight the upcoming SFPE PBD Conference, which will be held in Singapore in April. I can assure you that a large number of very interesting presentations will be delivered. I sincerely hope to see many of you at the event—please mark your calendars so you don't forget.

I will keep this final Editor's Column of the year short and simply say that I hope you enjoy these "Christmas gifts" from SFPE.

If any readers feel they have an important topic they would like to share with the industry, please do not hesitate to contact us—we would be happy to help make that happen.

As always, a sincere thank you to everyone who has dedicated significant time and effort to making this issue possible.

The next issue will be released in March.

Finally, I wish you all a very enjoyable holiday break.

Yours sincerely,

Jimmy Jönsson, Managing Editor

SFPE Europe Q4 2025 Issue 40

A Message from the SFPE Europe Chair

Dear SFPE Europe members and all those interested in Fire Safety,

A new chapter was born! SFPE Europe aims to encourage fire safety engineering founded on solid scientific principles. To achieve this, it helps establish new European SFPE Chapters. The latest addition, in North Macedonia, made a remarkable debut by organizing a Fire Safety Conference in Skopje on December 3-4, which attracted over 230 attendees from 23 nations. The conference featured invited speakers who shaped an engaging agenda.

Notably, four of these experts presenting at the conference came from the boards of other European SFPE chapters, highlighting the strength of the SFPE network across Europe. Kathrin Grewolls (SFPE Europe board, SFPE Germany chairman) spoke on fire risk analysis in urban areas. Gabriele Vigne (SFPE Spain treasurer) discussed CFD and tenability in fire and smoke modelling. Paulo Ramos (SFPE Portugal chairman, new SFPE Europe Board member) presented on EV charging stations in buildings and I covered the hot topic modern façades and fire. This highlight that under the SFPE umbrella we got a wide network of competences, and we are eager to spread this knowledge. The conference featured many excellent speakers, and the event was exceptionally well organized. Many thanks to Tatjana Vasiljevic Vladev, President of SFPE North Macedonia, for inviting us!

I'm truly grateful for the chance to serve as chairman of SFPE Europe over the past two years. Beginning January 1, 2026, I look forward to welcoming Wojciech Wegrzynski as the new chair for the 2026-2027 term.

Best regards,
Robert McNamee
SFPE Europe Chair

SFPE Europe's mission: "*SFPE Europe is leading the profession as a neutral, international non-profit organization to define, develop, and advance the use of fire engineering, fire protection*

engineering, and fire safety engineering best practices; expand the scientific and technical knowledge base; and educate the global fire safety community, in order to reduce fire risk."

Calibrating a 1D Tunnel Ventilation Model Using Real-World Data and AI Techniques: Application to a Large Urban Network

By: Fabián de Kluijver, JVVA, Spain, Alberto López, JVVA, Spain
Juan Manuel Sanz, Sener, Spain, Guillem Peris, Sener, Spain
Javier Berges, Madrid Calle 30, Spain, Mar Martinez, Madrid Calle 30, Spain

The present article offers a condensed synthesis of work previously presented at the 12th Tunnel Safety and Ventilation Conference (2024) [1], where the complete AI-supported field-data analysis and calibration workflow was described, and later in NAFEMS Benchmark magazine (July 2025) [2], which focused on the surrogate-modeling and calibration process.

1. Introduction

Ventilation design in road tunnels is essential for fire safety. During fire events, controlling smoke movement, maintaining tenable conditions for evacuation, and supporting firefighting operations depend on accurately predicting airflow under different operational and environmental conditions. In large infrastructures, this understanding relies increasingly on computational models, which must be carefully calibrated to reflect real behavior.

This article summarizes the calibration of a one-dimensional (1D) ventilation model for Madrid's M30 tunnel network, one of Europe's largest and most complex urban tunnel systems. The scale and heterogeneity of the network introduce uncertainties inherent to any physical model, making calibration a critical step. The availability of extensive field data provided a strong basis for refining predictions and reducing these uncertainties. To accomplish this, the project combined traditional engineering models, surrogate modeling, and artificial intelligence (AI) tools for data analysis. The resulting calibrated digital twin supports the development of both sanitary and fire ventilation strategies. Although centered on the M30, the methodology is applicable to other complex infrastructures where manual calibration is not feasible.

2. A Complex Urban Tunnel System

The M30 tunnel network forms a continuous underground ring around central Madrid. It includes 48 km of tunnels, equivalent to 118 km of single-lane roadway, with daily traffic exceeding 1.3 million vehicles.

The system incorporates 21 entrances, 22 exits, branching points, and widely varying cross sections. All of these elements contribute to a complex ventilation behavior resulting from the interaction between multiple interconnected tunnels.

The scale of the ventilation infrastructure further illustrates the system's complexity. As shown in Figure 1, the network includes nearly 1,000 ventilation fans and 684 environmental sensors, including 388 anemometers. This inventory shows the diversity of ventilation systems across the network, while the sensor deployment provides the monitoring capability needed for model calibration.
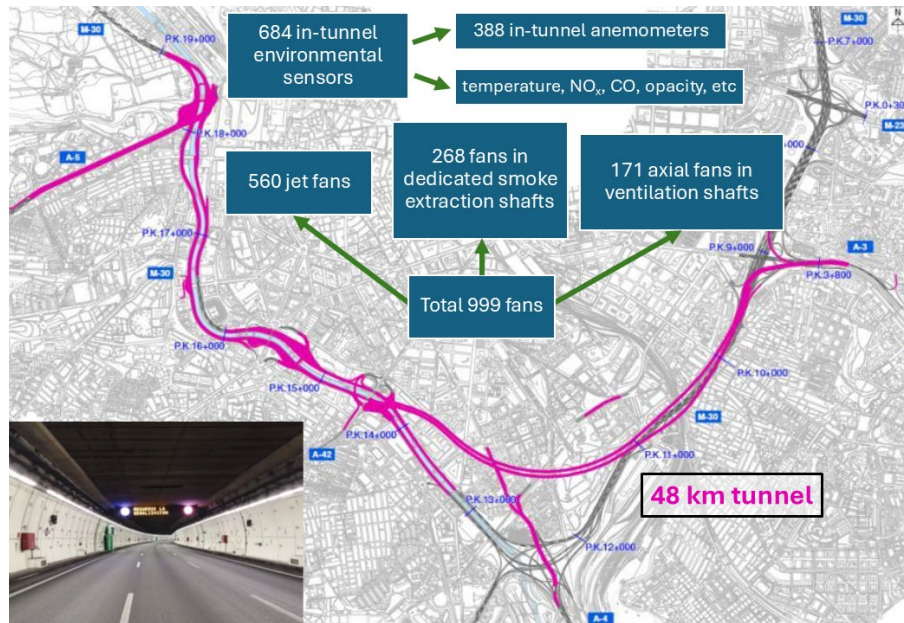

Figure 1. Map of the tunnel network, and list of tunnel ventilation equipment and air quality monitoring sensors.

3. Motivation and Objectives

With the tunnel's ventilation control equipment having reached the end of its useful life, a renewal project was started to ensure continued compliance with operational and safety requirements. This upgrade also provided an opportunity to reanalyze the existing ventilation approach and update the corresponding control algorithms. Improving these algorithms required an accurate understanding of airflow behavior under a wide range of operating conditions, motivating the development of a calibrated 1D ventilation model for the entire network.

Although three-dimensional fire simulations using Fire Dynamics Simulator (FDS) software were also conducted, these are limited to analyzing smoke movement in localized zones under predefined boundary conditions. They cannot represent the system-wide aerodynamic response to different equipment activation scenarios. A 1D model, on the other hand, can capture global flow balances, pressure losses, heat transfer effects, and interactions between ventilation equipment across the full network. The main objective of this work was therefore to develop and calibrate such a model using field data.

4. Preparing and Understanding Field Data Through AI

Processing the M30's field data required a dedicated methodology. Over the last decade, more than three terabytes of operational data have been recorded by the control center, including traffic information, anemometer readings, environmental measurements, and equipment states. The scale and heterogeneity of this dataset made manual processing unmanageable, requiring the use of AI-assisted tools.

The first step was data homogenization, removing periods not representative of normal operation such as fire drills, equipment faults, or sensor malfunctions. AI routines compared each sensor to its neighbors to detect anomalies and improve dataset consistency. Clustering and pattern-recognition techniques then grouped anemometers with similar temporal behavior, revealing aerodynamic zones within the network and providing a clearer understanding of how different areas respond to traffic, natural draft, and thermal conditions.

AI analysis also quantified relationships between traffic flow, vehicle speed, and air velocity, clarifying the role of the piston effect. Temperature records showed how natural draft relates to external weather, influencing airflow direction and magnitude. In addition to cleaning and characterizing the data, these AI-based methods provided valuable tools for visualizing and analyzing ventilation behavior across different areas and operating conditions, improving the system-level understanding needed to interpret field data for model calibration.

5. The One-Dimensional Ventilation Model

The ventilation model was implemented using IDA-Tunnel [6], a simulation tool widely used in the design of railway and road tunnel networks around the world, and validated through several studies [7], [8]. A 1D model is appropriate when longitudinal dimensions far exceed transverse ones: flow variables vary along the tunnel axis but are assumed uniform across each cross section. Although simplified, this approach effectively models the global airflow behavior at reduced computational cost, including fluid phenomena such as pressure losses, vehicle-induced piston effects, pollutant transport, and thermal influences.

The M30 tunnel network model comprises 194 interconnected tunnel segments between portals, branches, and connections to ventilation shafts, as illustrated in Figure 2. Depending on the sector, the model represents longitudinal, transverse, or semi-transverse ventilation, reflecting the ventilation configurations present in the infrastructure.

For this study, the simulation model inputs are grouped into two categories:

- **Model parameters (θ):** inputs to the model that remain constant over time and whose values carry an associated uncertainty. In this study, these parameters include friction coefficients, representative cross-section heights, vehicle aerodynamic coefficients, and a wall-temperature-related parameter introduced to compensate for steady-state simplifications.

- **State inputs (x):** time-varying quantities measured in the field. In the model considered, these inputs correspond to traffic flows in each tunnel segment and the ambient temperature. For this study, they are assumed to be known from field data, and no uncertainty is assigned to them.

Calibration focused on determining the values of the model parameters (θ) that minimized the discrepancy between simulated and measured air velocities across the network's anemometers.
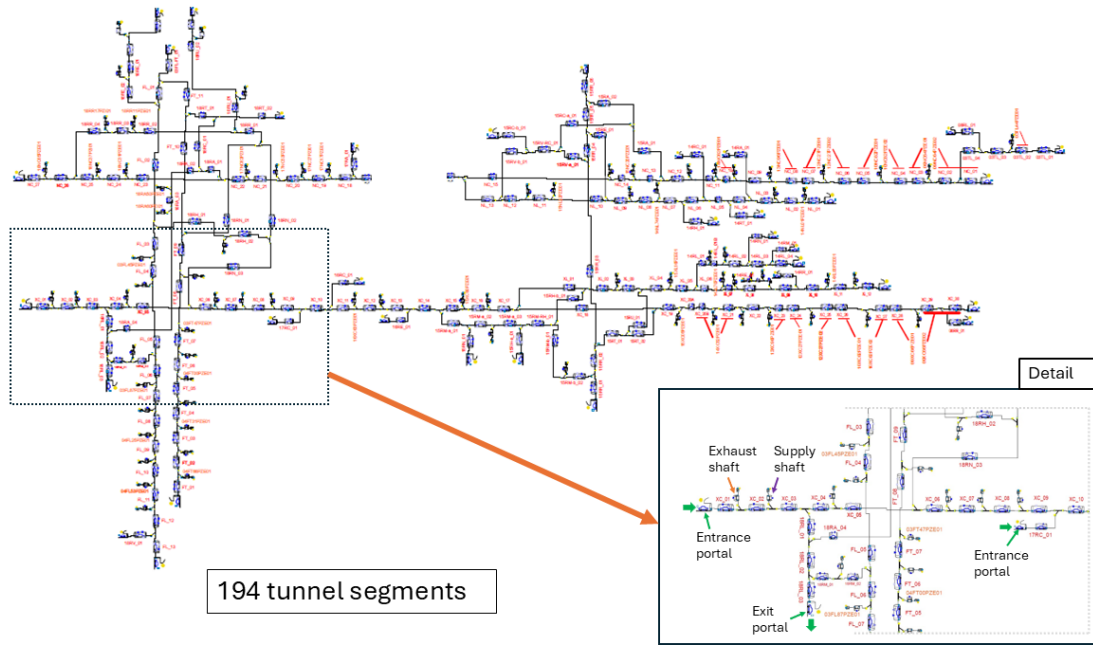
Figure 2. Diagram of the 1D simulation model.

6. Calibration Methodology

6.1 Calibration Framework

Some of the available field data correspond to state inputs of the model, such as traffic flow and ambient temperature. Other variables measured in the field correspond to model outputs, including air velocity at different anemometers and temperature within the tunnels. This relationship between model inputs, model outputs, and the available field data is illustrated in Figure 3.

Assessing how accurately the model reproduces real airflow behavior requires a systematic method. In this study, air velocity is selected as the output variable for calibration, since it is measured throughout the network by hundreds of anemometers and provides a direct indicator of the system's behavior. For each combination of model parameters (θ) and state inputs (x), the 1D model generates predicted air velocities at all anemometers. These predictions are compared with field measurements, producing error values across a wide range of operating states. Individual errors are then combined into a global error metric that depends only on θ.

The calibration process consists of an optimization process that aims to find the θ values that minimize this metric. To carry out this task, the calibration process needs to explore the parameter space by comparing simulation outputs with field data across many different combinations of model parameters and state inputs. This exploration seeks the parameter set that provides the best overall agreement with the measurements. Since such an extensive search cannot be performed manually, an automated method is required to efficiently evaluate and refine candidate parameter sets. Achieving this relies on an iterative optimization procedure in which successive candidates are tested and progressively improved until the convergence criteria are met. In this project, a differential evolution algorithm [3] was selected for the optimization process because of its ability to explore high-dimensional parameter spaces effectively and avoid convergence to local minima (global optimization). An overview of this iterative process and its structure within the calibration workflow is shown in Figure 4.

For the calibration, the focus was placed on periods without mechanical ventilation, when airflow is driven only by traffic (piston effect) and thermal differences (natural draft). To ensure that only these

natural-ventilation conditions were used, field data corresponding to any hour in which jet fans or extraction shafts were active was filtered out. The dataset used for calibration covered an entire year of measurements, specifically the most recent full year available: 2021, which contains 8,760 hours of recorded data. After removing all periods with active ventilation equipment, a total of 3,884 hours remained. Each of these hours was treated as a quasi-steady-state period in which traffic flow and ambient temperature were assumed constant, allowing the calibration to focus on average system behavior rather than transient effects. Although no two hours present exactly the same traffic and temperature values, the system state tends to repeat in an approximate manner throughout the year, giving rise to groups of state input vectors that are very similar and can be expected to induce similar airflow conditions in the tunnels. For this reason, these hours were grouped into 500 representative clusters in order to preserve variability while reducing computational load during the optimization process.
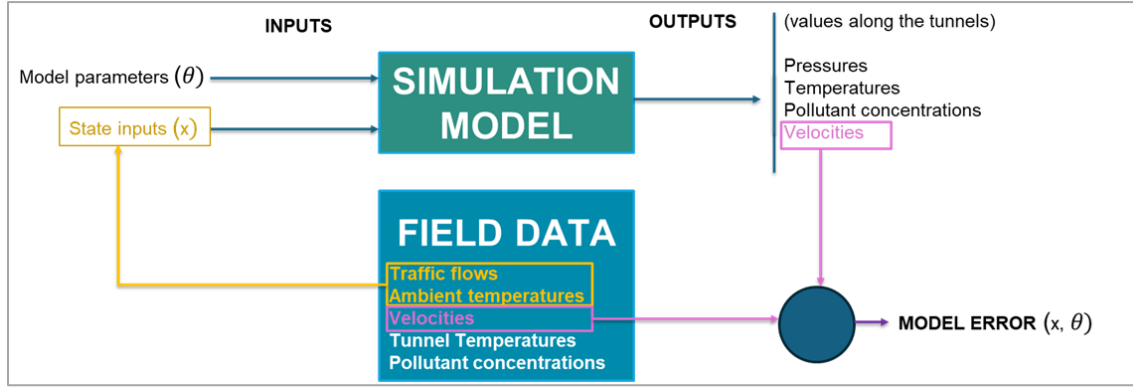

Figure 3. Diagram of relationships between model inputs, model outputs, field data, and calculation of model error.
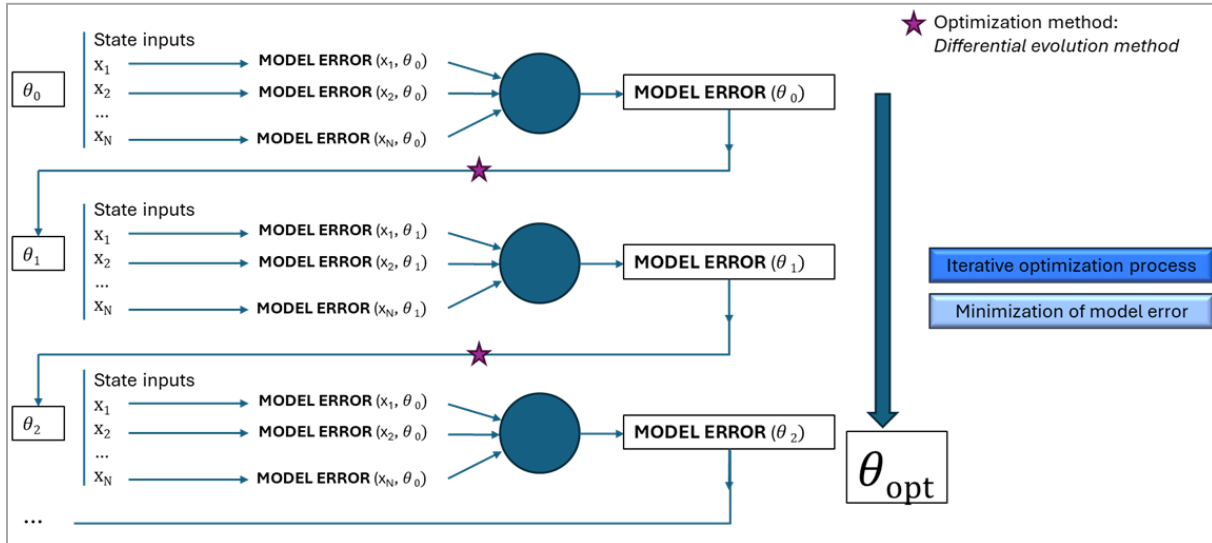

Figure 4. Diagram of calculation of global model error and representation of the calibration process as an iterative optimization method over the parameter vector.

6.2 Computational Cost and Surrogate Modeling

Taking into account that each 1D simulation requires approximately 20 seconds and that each optimization iteration needs to evaluate 500 representative operating states, a single iteration of the calibration process would take roughly 2.8 hours to complete. Since an optimization process of this type typically requires hundreds of iterations to reach convergence, the total computation time would quickly become unmanageable.

To address this computation time issue in the calibration process, a surrogate model of the 1D simulation was developed. A surrogate model is a simplified mathematical representation designed to reproduce the outputs of a complex simulation model while requiring significantly less computation time. In this project, the surrogate was built to predict air velocities at all anemometer locations for any given combination of model parameters θ and state inputs x, closely emulating the behavior of the 1D simulation under steady-state no-ventilation conditions.

The regression model selected for the surrogate is a commonly applied machine-learning method: a regression tree model, specifically a gradient-boosted regression tree [4], [5]. A set of 3,000 simulations was run directly using the 1D simulation model, by varying both θ and x across the calibration space, and the resulting air velocities were used to train a separate surrogate model for each anemometer. Together, these individual models formed the surrogate that was used throughout the calibration process.

The accuracy of the surrogate was assessed by comparing its predictions with those of the 1D model. The R^2 distribution across anemometers, shown in Figure 5, indicates consistently high values, confirming that the surrogate provided a reliable approximation of the simulation outputs. The computational gains were substantial: the evaluation time per simulation decreased from about 20 seconds to approximately 0.07 seconds. As a result, the duration of each optimization iteration decreased from roughly 2.8 hours to about 35 seconds, making it possible to perform the repeated evaluations required by the optimization algorithm within realistic engineering timeframes.

With this surrogate-based framework in place, the optimization can be carried out efficiently. The calibration algorithm repeatedly evaluates the surrogate instead of the full 1D model, which enables rapid exploration of the parameter space. The process continues until the convergence criteria are met, resulting in a calibrated digital twin of the infrastructure's ventilation system.
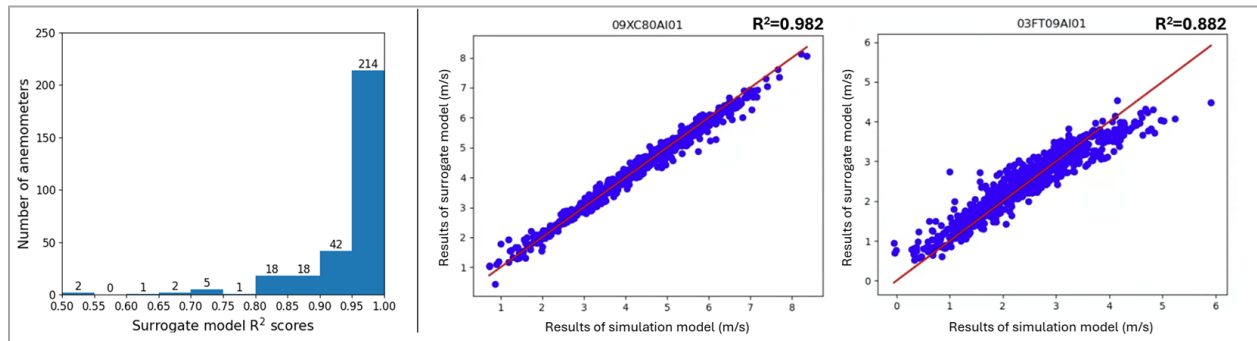

Figure 5. Left - General performance of surrogate model represented as a histogram of R2 scores of the surrogate models of each of the anemometers. Right - Example of performance of surrogate model of two of the anemometers considered. Predictions of surrogate models compared against result of the simulations.

7. Calibration Results

The calibration improved the model's ability to match real system behavior. Figure 6 illustrates this improvement under conditions without mechanical ventilation, showing how the calibrated model more accurately captures both the magnitude of air velocity and its dependence on traffic flow (piston effect). At a global scale, Figure 7 shows the reduction in prediction errors across anemometers after calibration, confirming the enhanced agreement between simulated and measured airflow. These results demonstrate that the calibrated model reliably reflects the aerodynamic behavior of the system.
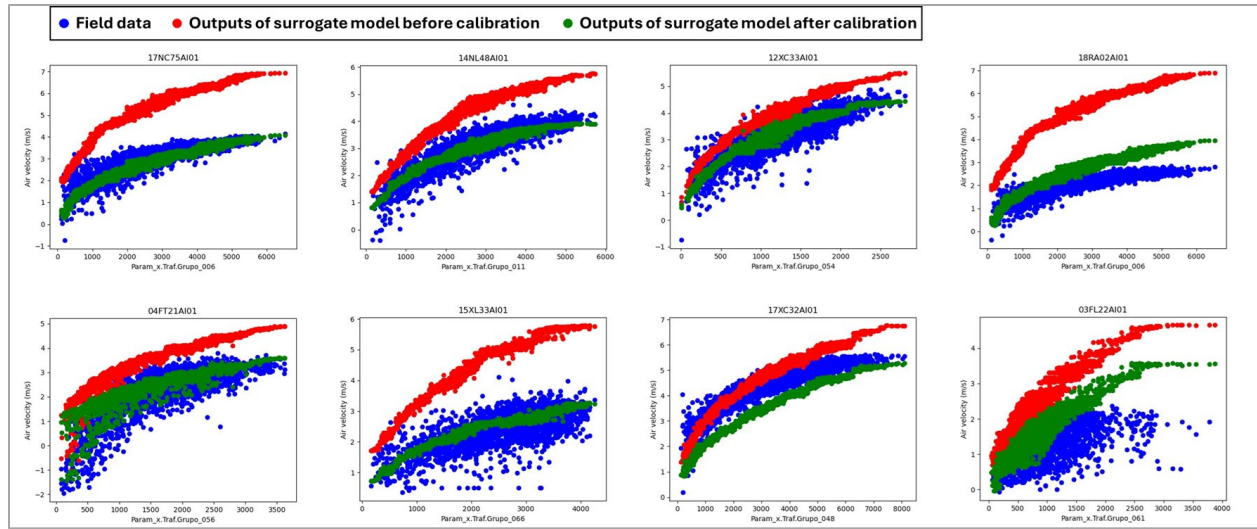
Figure 6. Air velocity (m/s) for different anemometers against the traffic flow (vehicles/hour) in the tunnel segment where the anemometer is placed. Three data sets are represented for each anemometer, field data (blue dots), outputs of surrogate model before calibration (red dots), and outputs of surrogate model after calibration (green dots).
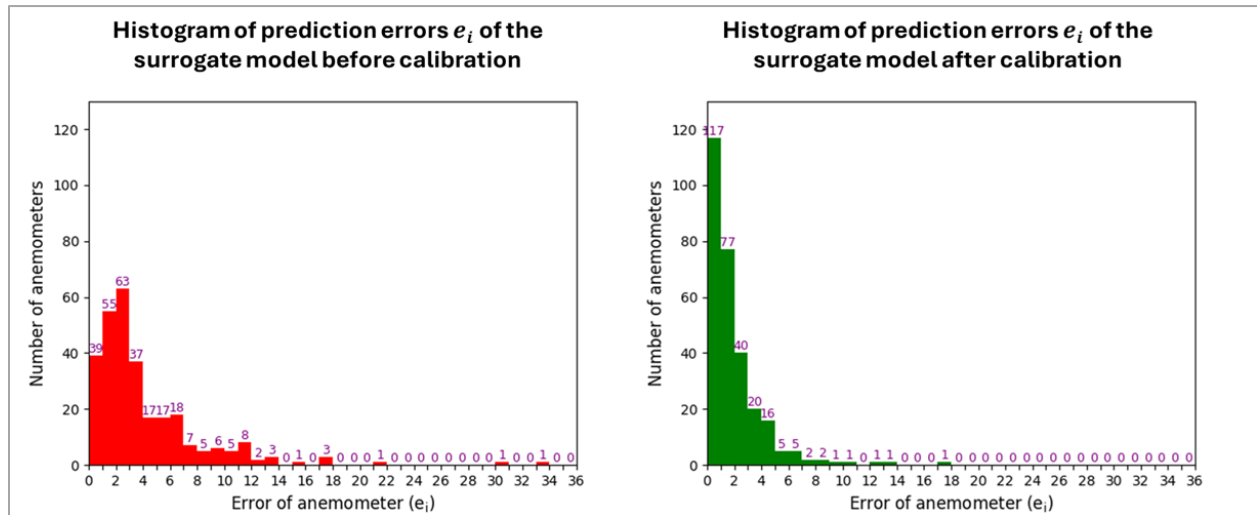

Figure 7. Histograms of the distribution of errors of the surrogate model in the prediction of field data. Left – Before calibration. Right – After calibration.

8. Validation Under Mechanical Ventilation

A second validation phase addressed mechanical ventilation. In this case, the calibrated model was evaluated using controlled on-site tests involving the activation of jet fans and extraction shafts. These scenarios were simulated and compared with the corresponding measured airflow responses. Agreement was strong, with only minor adjustments required to fan efficiencies and shaft parameters. This confirmed that a model calibrated under natural-ventilation conditions can also accurately represent mechanically driven airflow.
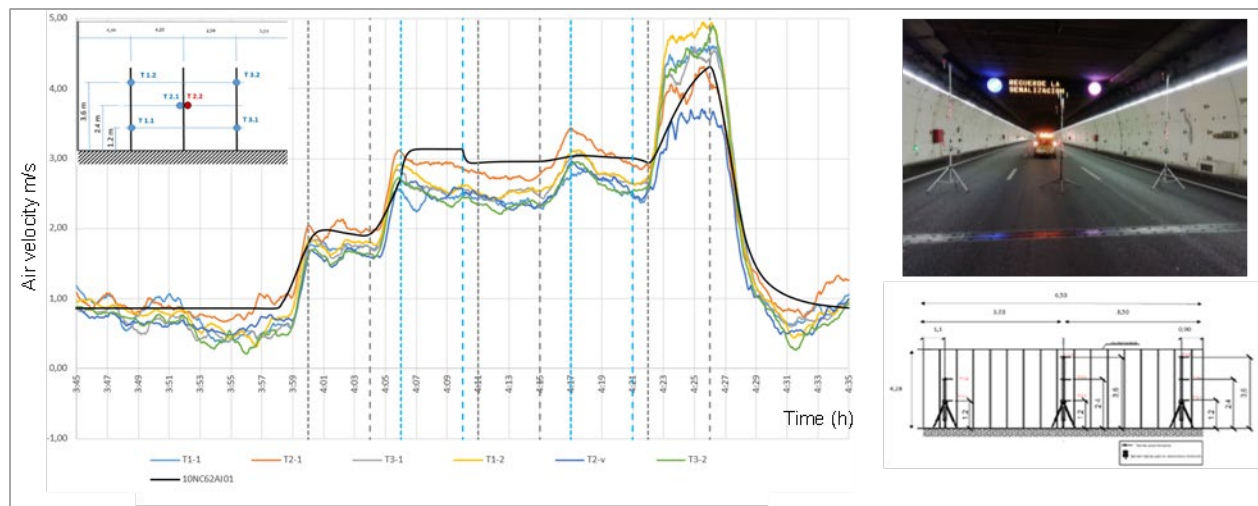
Figure 8. Results of air velocity results obtained in one of the aerodynamic tests. Comparison of simulation results (10NC62AI01 line) with the measurements of the six anemometers used in the test (T1-1, T2-1, T3-1, T1-2, T2-v, T3-2).

9. Application to Ventilation Strategies

After calibration, the model was used to evaluate a wide range of ventilation strategies by simulating different equipment activation scenarios. These simulations provided the basis for defining updated operational algorithms for both fire and sanitary ventilation.

For fire ventilation, the strategies developed aimed to limit the area affected by smoke, prevent spread into adjacent tunnels or branches, and maintain adequate upstream airflow to preserve stratification and avoid backlayering. The calibrated model allowed evaluating these objectives under different fire scenarios to determine the most effective combinations of ventilation equipment for each fire scenario analyzed.

For sanitary ventilation, referring to the control of pollutants generated by day-to-day traffic, the model helped identify equipment configurations capable of maintaining acceptable air quality while optimizing energy use. By exploring many combinations of jet fans and shafts, the model clarified where ventilation is truly needed and where it can be reduced without compromising environmental conditions.

These results have been used to define the ventilation algorithms that will be implemented in the M30 control center. Their performance will be evaluated through full-scale aerodynamic and smoke tests in upcoming project phases.
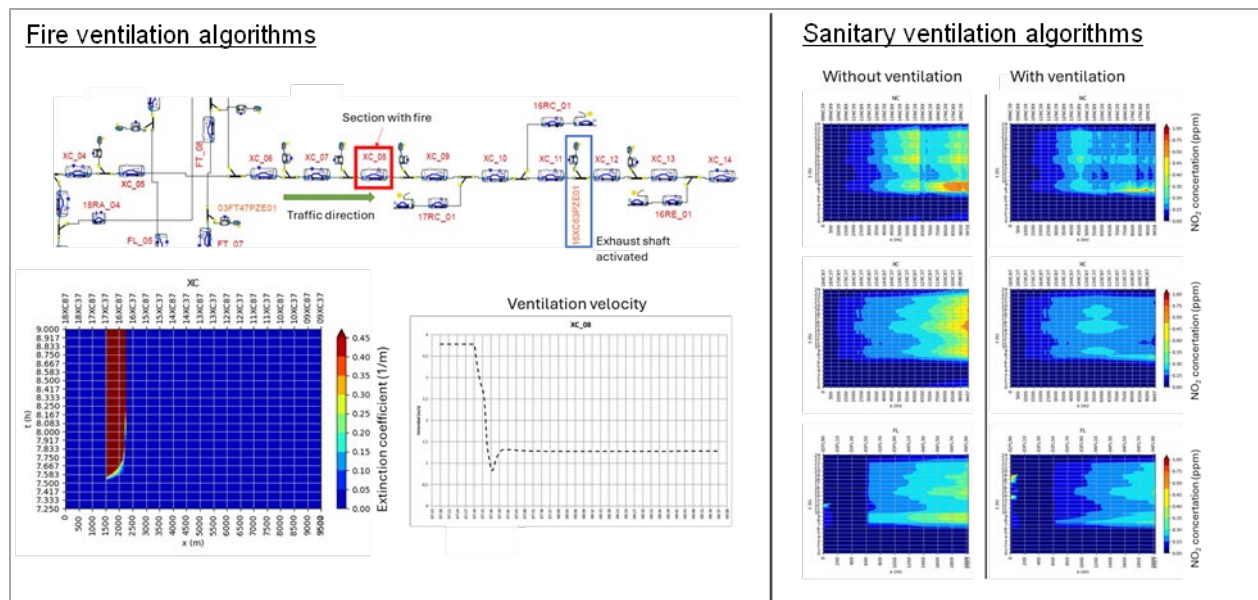
Figure 9. Left - Example of a fire ventilation calculation (fire located in tunnel segment XC_08) performed using the calibrated 1D model. Diagram (top); smoke propagation along the tunnels (bottom left); ventilation velocity (bottom right). Right - Example of a sanitary ventilation calculation performed using the calibrated 1D model. Representation of evolution of NO_2 concentration along three tunnels NC, XC, and FL.

10. Conclusions

Physical models inevitably contain uncertainties in their parameters and assumptions, and these uncertainties become particularly significant in systems with many interconnected elements and large numbers of parameters. Calibration is therefore essential to obtain a robust and reliable model that reflects real behavior. For a system as extensive and complex as the M30 tunnel network, where airflow is influenced by numerous interacting components, meeting this challenge required a methodology combining physical modeling, surrogate-based optimization, and AI-driven data analysis.

The high dimensionality of the parameter space made direct calibration computationally infeasible. This difficulty was overcome by developing a surrogate model capable of reproducing the 1D simulation's behavior with drastically reduced computation time. This approach enabled efficient exploration of the parameter space, making an iterative optimization process, otherwise unmanageable, viable within real project constraints. The result is a calibrated digital twin that accurately represents system behavior and provides a solid foundation for designing ventilation strategies. The ability to complete this process within realistic time and resource limits demonstrates the practical applicability of the methodology beyond academic contexts.

More broadly, the work highlights the value of integrating engineering expertise with data-driven methods. As tunnel infrastructures become more instrumented, such approaches could support future advances in model calibration, operational optimization, and fire-safety planning. This analysis was made possible thanks to the historical data recorded by the M30 control center, emphasizing the importance of equipping infrastructures with appropriate sensor instrumentation and ensuring that measurements are reliably stored for long-term use.

Methodologies that blend physical modeling with surrogate models and AI techniques offer a promising path for the evolution of fire-safety engineering in complex infrastructures. By enabling models that are both computationally efficient and tightly anchored to real system behavior, they provide practitioners with powerful tools to support design decisions, improve operational strategies, and strengthen resilience across modern tunnel networks.

References

[1] Sanz, J. M., De Kluijver, F., López de Arriba, A., Berges, J., Martínez, M., & Peris, G. (2024). Application of AI to the 1D Ventilation Analysis of a 43 km Complex Road Tunnel Network: Madrid Calle30. In: Proceedings of the 12th International Conference on Tunnel Safety and Ventilation. Graz, Austria: Graz University of Technology.

[2] De Kluijver, F., López, A., Sanz, J. M., Peris, G., Berges, J., & Martínez, M. (2025). Application of Machine Learning for Surrogate Modeling: Calibration of a 1D Ventilation Model of a Complex Road Tunnel Network. NAFEMS Benchmark Magazine, July 2025.

[3] SciPy, "*scipy.optimize.differential_evolution — SciPy v1.12.0 Manual*." [Online]. Available: https://docs.scipy.org/doc/scipy/reference/generated/scipy.optimize.differential_evolution.html. Accessed: June 11, 2025.

[4] F. Pedregosa, G. Varoquaux, A. Gramfort, *et al.*, "Scikit-learn: Machine learning in Python," *J. Mach. Learn. Res.*, vol. 12, pp. 2825–2830, 2011.

[5] Scikit-learn, "*1.11. Ensembles: Gradient boosting, random forests, bagging, voting, stacking*." [Online]. Available: https://scikit-learn.org/stable/modules/ensemble.html#gradient-boosting. Accessed: June 11, 2025.

[6] Equa Simulation AB, *IDA-Tunnel for Rail and Metro Tunnels*. [Online]. Available: https://www.equa.se/en/tunnel/ida-tunnel/rail-metro-tunnels. Accessed: June 11, 2025.

[7] P. Sahlin, L. Eriksson, P. Grozman, H. Johnsson, and L. Ålenius, *1D Models for Thermal and Air Quality Prediction in Underground Traffic Systems*, Equa Simulation AB, Sweden.

[8] P. Särkkä, *Tunnelling Market in Finland*, Chairman, Scientific Committee, WTC2011, Helsinki, Finland.

Understanding Fire Dynamics in Open Car Parks: Insights from Multiparametric CFD Analysis

By: Wojciech Węgrzyński, ITB, Poland, Jakub Bielawski, ITB, Poland

Danny Hopkin, OFR, UK, Michael Spearpoint, OFR, UK

Introduction

Recent fire incidents in multi-storey car parks have renewed focus on understanding the mechanisms governing fire spread between vehicles and the influence of structural design parameters on fire severity. In recent decade in nearly every year over the past decade there has been a major car park fire, which either resulted in a complete demolition of the structure, or lead to a long repair progress. Previously Tohir et al. (2018), and more recently Miechówka and Węgrzyński (2025) have summarized those in a recent literature review. While several large-scale experimental programmes, including the BRE (2010) study, have provided valuable empirical data, the complexity of vehicle fire development and interaction with the built environment continues to challenge design assumptions. It can be argued that the set of conditions that promote a growth of the fire from a localized event with a few vehicles into a conflagration impacting the building is a topic of continued interest. We attribute those conditions to include car park floor-to-floor height, vehicle occupancy rate, the size of the vehicles, the influence of the external wind conditions. However, we lack a complete explanation on the fire spread mechanisms in large fires, that would provide context on which these variables play a critical role.

Table 1. Examples of large car park fires based on media reports, 2017 – 2024, Miechówka and Węgrzyński (2025)

City, Country	Approx. number of cars involved	Description	Year
Engelen, Netherlands	50	Under residential complex	2024
Atsugi, Japan	100	Free standing car park	2023
Munich, Germany	29	Free standing car park	2023
Luton, England	1500	Airport	2023
Marsta, Sweden	200	Residential car park	2021
Warsaw, Poland	50	Under residential complex	2020
Stavanger, Norway	300	Airport	2020
Cork, Ireland	60	Above shopping mall	2019

New York, USA	120	Kings Plaza shopping mall	2018
Liverpool, England	1150	Next to a sports arena	2017

To address the uncertainties, the Fire Research Department at the Building Research Institute (ITB) in Warsaw in collaboration with OFR Consultants in the UK conducted a multiparametric computational fluid dynamics (CFD) analysis to investigate how key geometrical and environmental variables affect fire growth in multi-storey car parks. The study employed the ANSYS Fluent CFD model with automated model creation and data processing scripts, to explore the combined effects of ceiling height, structural bay configuration, arrangement of parked vehicles, and external wind conditions on fire behaviour. The investigated outcomes were predominantly the heat flux at a distance from burning vehicles as this would likely lead to further fire spread.

The research sought not only to enhance the scientific understanding of the phenomenon but was also the first step informing the further development of simplified cellular automata models that could support extensive parametric engineering assessments and regulatory decision-making for multi-storey car parks.

Methodology

The CFD analyses were performed using ANSYS Fluent software (v 19.1), with transient, pressure-based solver with the unsteady Reynolds-averaged Navier–Stokes (URANS) turbulence model and the Eddy Dissipation Model (EDM) for combustion. Heat transfer through convection, conduction, and radiation was fully resolved using the discrete ordinates radiation model and the weighted-sum-of-gray-gases (WSGGM) approach.

Preliminary calibration of the CFD framework was undertaken against Experiment 1 from the BRE fire spread programme, which investigated heat flux and flame propagation between three passenger vehicles. The CFD model reproduced the experimental geometry and fire development profile, achieving close agreement in peak surface heat flux (CFD: ≈115 kW/m²; experiment: ≈100 kW/m²). While some discrepancies were noted, principally due to simplifications in vehicle geometry, the validation confirmed that the numerical approach could reliably represent the early and fully developed stages of vehicle fires and heat flux distribution from both the vehicle fire plume, as well as the ceiling jets and the hot smoke layer. Some of the simulation findings are illustrated in Figure 1.

Following the calibration, a model of a car park was built representing a typical UK open car park solution, in which we have performed a systematic sensitivity analysis comprising 31 individual transient simulations was performed to evaluate the influence of:

- presence of the structural bays (beamed vs. flat-ceiling configurations),

- location of the parked vehicles in relationship to the structural layout of the beams,

- car park ceiling height (2.5 m – 3.3 m),

- number of burning vehicles (one to three), and

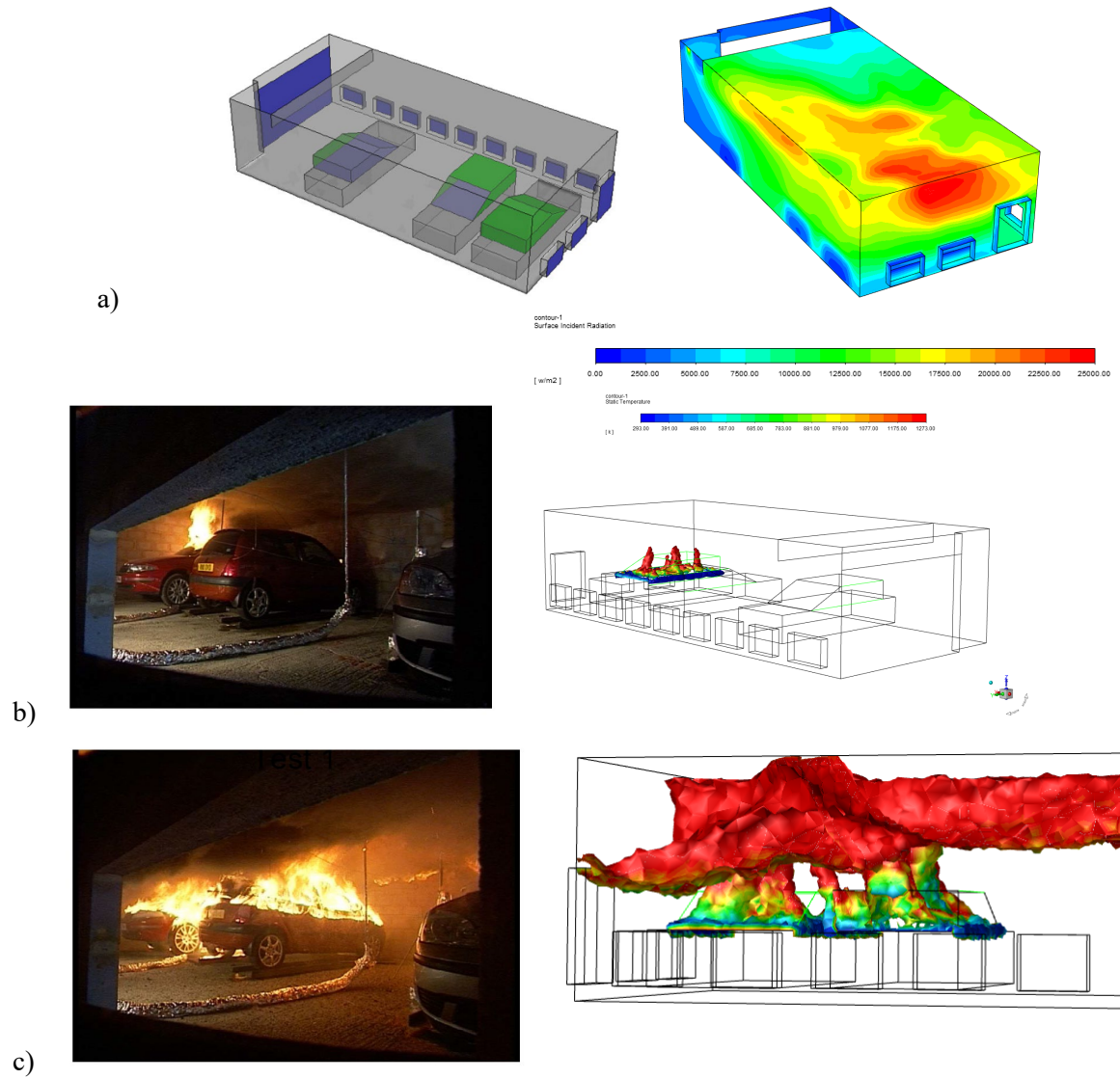- vehicle orientation (parallel or perpendicular to structural bays).

Fig. 1.
(a) numerical model and the distribution of the heat flux in 12th minute of the CFD simulation, (b) comparison of the flame shape in 6th minute of the BRE (2010) experiment with contours of flame (iso-contour of stoichiometric fuel to air ratio) in the corresponding time, (c) at the 21st minute of the BRE (2010) experiment

A simplified representative fire growth was prescribed as a linearly increasing heat release rate (HRR) up to 15 MW over 15 minutes. Boundary conditions simulated open façades typical of naturally ventilated car parks. While the conditions promoting transition to a conflagration were investigated for a range of HRRs, in this short paper we present the most relevant results for chosen values of HRR corresponding to fires which in some circumstances could spread beyond the initial burning vehicles.
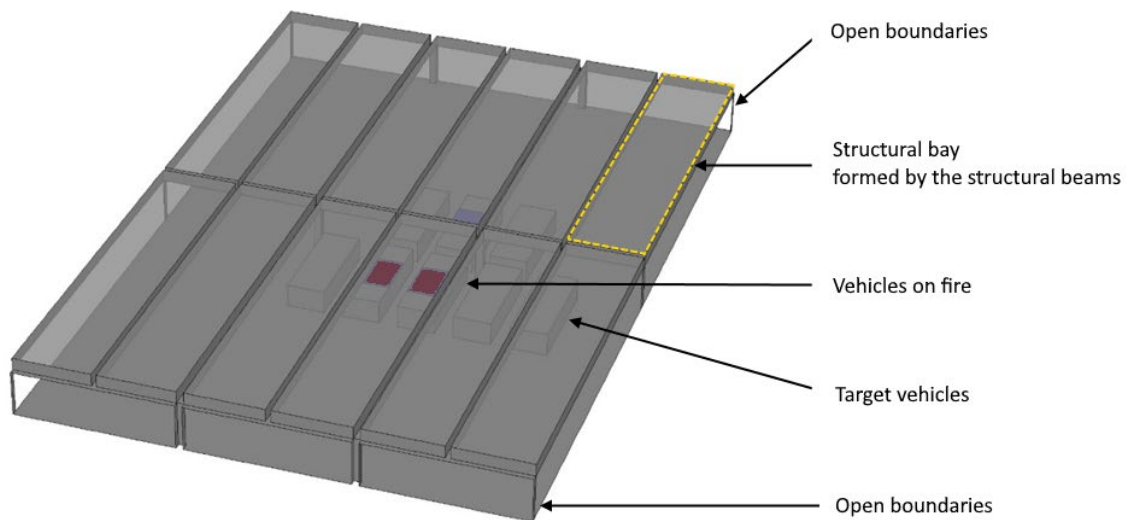
Fig. 2.   Model of the car park used in the parametric study

Key Findings

Structural Bay Effect

One of the most significant findings was the structural bay effect - the influence of structural beams in constraining flame extension under the ceiling. This follows a previous observation by Deckers et al. (2013), who observed similar results in relationship with smoke control. CFD results revealed that beams form quasi-compartments in which flames are trapped, leading to elevated ceiling temperatures (up to 920 °C) and heat fluxes exceeding 25 kW/m² towards the floor. When considering classical approach to radiation from fires, as in Heskestad (1983), the heat flux resulting from the flame extension may be higher than the one from the flame, at distances of a few metres.

In contrast, when structural elements were removed and the ceiling was flat, the flames assumed a more axisymmetric form, ceiling temperatures were substantially lower, and radiation to adjacent vehicles decreased markedly. The presence of structural bays thus promotes localized fire severity and enhances the likelihood of lateral fire spread within, rather than between, bays.
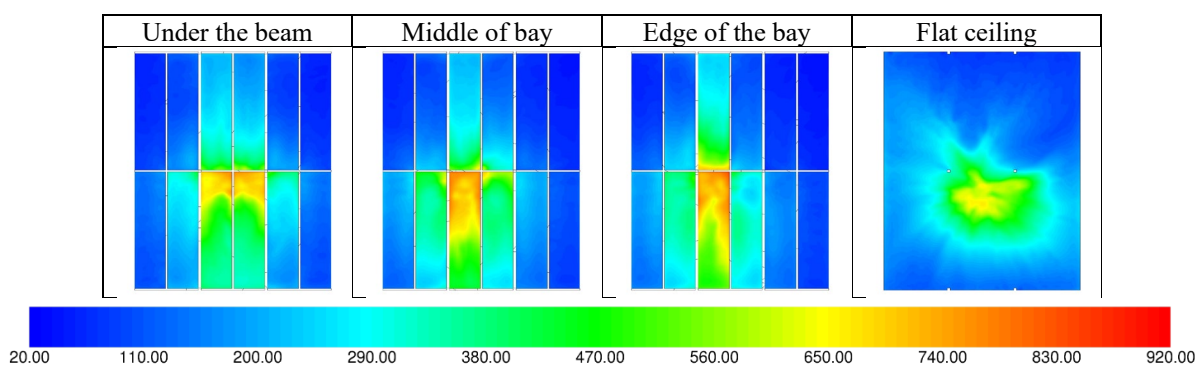

Fig. 3.   Temperature of the exposed ceiling surface for different locations of the fire within the structural bay, and compared with the flat ceiling configuration. Results for 8 MW fire

Influence of Ceiling Height

Ceiling height was found to be a dominant parameter in determining whether flames impinge on the ceiling and form a flame extension underneath the ceiling, or there is only a smoke ceiling jet. In low car parks (2.5 m), flames from an 8 MW vehicle fire readily reached the ceiling, producing extensive

flame spread beneath structural beams. Increasing the height to 2.9 m or 3.3 m reduced or eliminated this extension, leading to lower surface heat fluxes on the adjacent targets and slower potential fire spread.

This observation supports the hypothesis that in car parks with sufficiently high ceilings, flame extensions are less likely to form, thereby reducing the probability of secondary vehicle ignition. The study illustrates that for a given HRR, the fraction of combustion occurring in the ceiling jet diminishes as height increases, with most heat release confined to the fire plume region.

Table 2 summarizes the HRR at which vehicles up and downstream from those burning, i.e. A and B would ignite assuming a critical heat flux for ignition of 15 kW/m^2. The HRR represents the 5th percentile, meaning that in 95% of cases the critical heat release rate to exceed 15 kW/m^2 would have been higher.

a)

b)
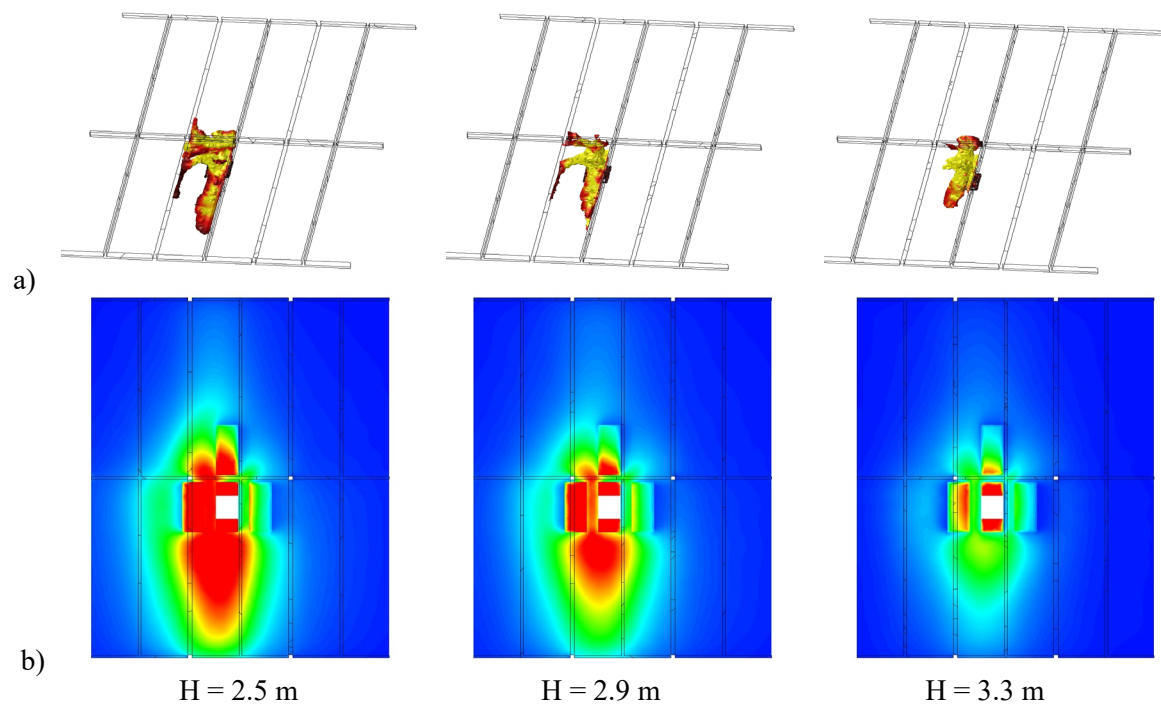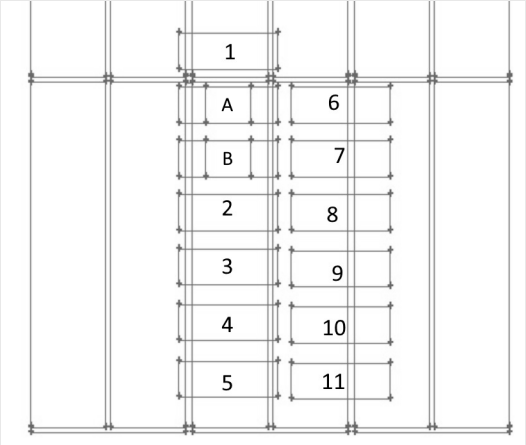
| H = 2.5 m | H = 2.9 m | H = 3.3 m |

Fig. 4.   Results of the single vehicle fire with HRR of 8 MW with structural elements for car park with height of 2.5 m, 2.9 m and 3.3 m, (a) flame shape, (b) Incident radiation at floor (0 – 25 kW/m²)

Table 2. Critical heat release rates (MW) for car ignition in function of ceiling height (A & B represent the ignited vehicles)

Car pos.	Range of critical heat release rate [MW] in function of ceiling height (5th percentile)			
	2.5 m	2.9 m	3.3 m	
1	3.61-4.82	3.68-6.59	4.46-7.56	
2	3.04-4.84	3.88-5.73	5.06-5.84	
3	3.41-5.85	4.32-7.13	5.69-7.10	
4	4.21-6.19	4.75-8.00	6.15-8.05	
5	5.37-6.80	5.33-8.58	6.32-8.51	
6	4.59-5.38	5.42-5.91	5.19-8.82	
7	5.22-5.80	5.72-5.96	5.68-6.43	
8	6.24-6.72	5.80-6.57	6.44-7.28	
9	6.89-7.78	7.08-7.94	7.18-8.31	
10	7.16-8.52	7.31-8.53	8.34-8.99	
11	7.17-10.23	7.60-9.43	8.58-9.36	

Multiple-Vehicle and Orientation Effects

When multiple vehicles burned simultaneously, the distribution of HRR between fire plumes and ceiling jets became spatially complex. A 12 MW scenario involving three vehicles produced a more uniform temperature field but slightly lower peak heat fluxes to the floor than a single 12 MW vehicle fire, as energy was distributed over a larger area.

Vehicle orientation also played a measurable role. Aligning vehicles perpendicular to structural bays led to higher incident heat fluxes on adjacent targets, especially when multiple plumes merged beneath a beam. This indicates that vehicle arrangement relative to the structural frame can materially affect the rate and direction of fire spread. Again, different results were observed for higher car parks, where in general – greater floor to ceiling height resulted in a lower heat flux to the fire surroundings, and less pronounced "bay effect".

H = 2.5 m

One vehicle   Two vehicles   Three vehicles

H = 2.9 m

One vehicle   Two vehicles   Three vehicles

H = 3.3 m

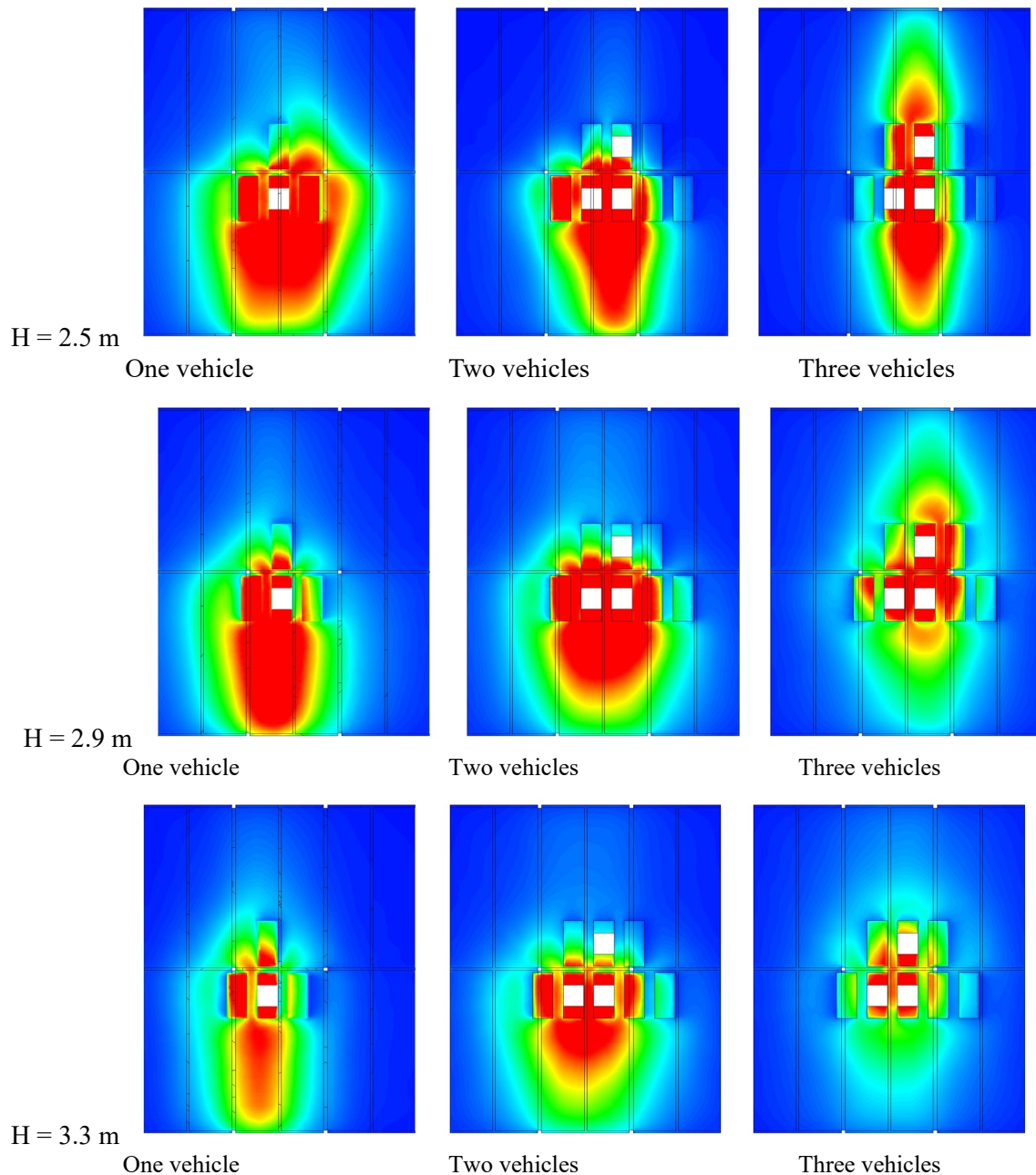One vehicle   Two vehicles   Three vehicles

Fig. 5.   Results of one, two or three vehicle fire with HRR of 12 MW with structural elements for car park with height of 2.5 to 3.3 m. Incident radiation at floor (0 – 25 kW/m²)

<u>Wind Influence</u>

To explore environmental variability, supplementary simulations incorporated external wind velocities of 2, 4, and 8 m/s applied laterally across the car park. Even low wind speeds of 2 m/s significantly altered smoke flow and flame geometry. While increased external wind-induced ventilation generally reduced ceiling-level heat flux—through enhanced mixing of hot gases with fresh air—an external wind also caused flames to tilt and extend horizontally, increasing the likelihood of direct flame contact with neighbouring vehicles.
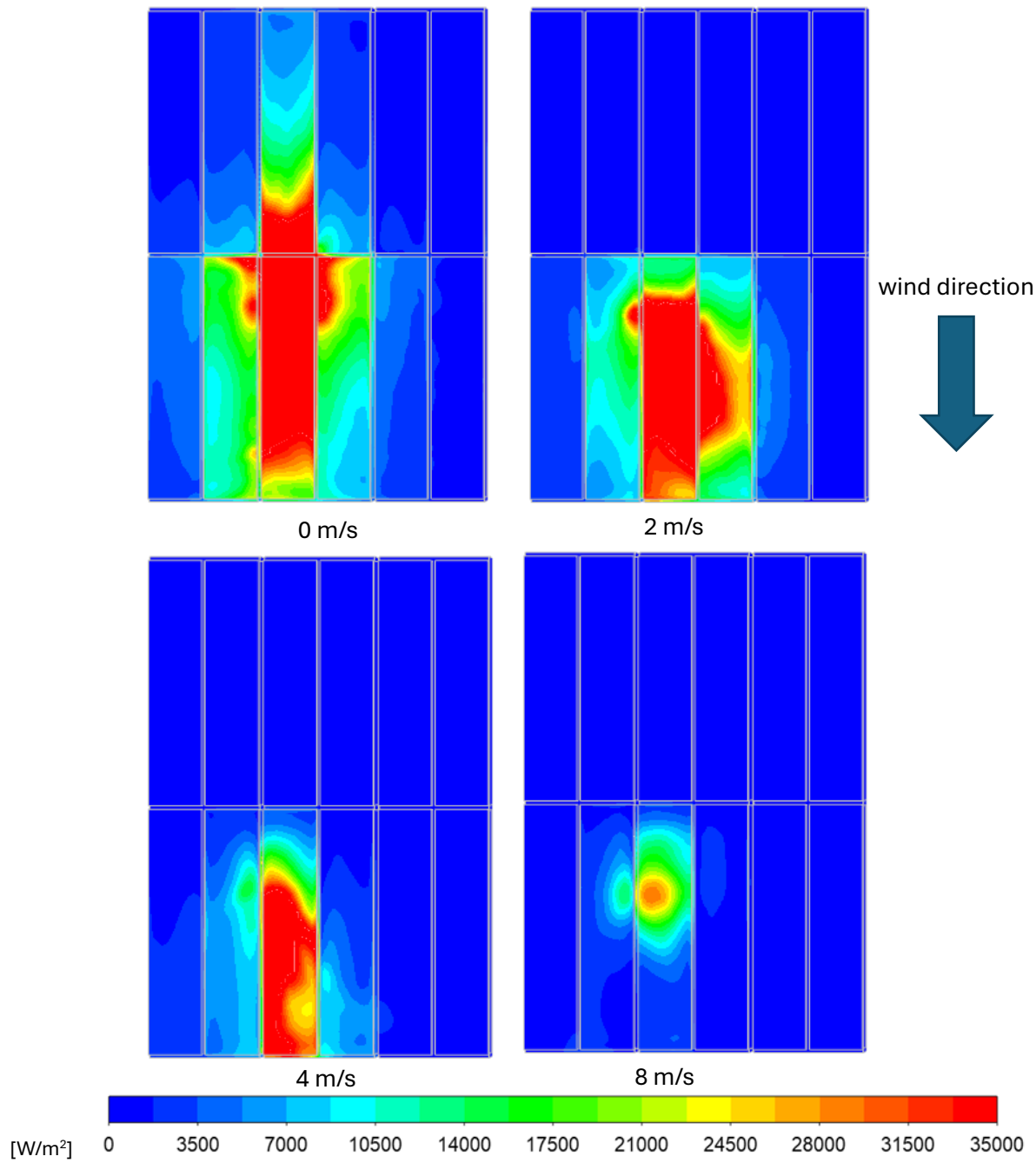
wind direction

0 m/s

2 m/s

4 m/s

8 m/s

[W/m²]   0   3500   7000   10500   14000   17500   21000   24500   28000   31500   35000

Fig. 6.   Radiation contours on the car park ceiling of 2.5 m height, at 8 MW fire and different wind velocities

Discussion

From the combined analyses, we have observed strong influence of the presence of flame extensions under the ceiling on the resulting potential for fire spread. Four working hypotheses have been formulated related to the governing physical phenomena influencing the presence of this flame extension within open car parks:

1. **Energy Distribution Hypothesis:** For a given geometry, only a limited portion of the total HRR can be accommodated within the fire plume. Excess energy manifests as a flame extension under the ceiling.

2. **Height-Dependence Hypothesis:** Increasing the vertical clearance between vehicles and the ceiling reduces the likelihood of flame extensions and therefore the likelihood of vehicle-to-vehicle spread.

3. **Bay Confinement Hypothesis:** Structural elements that constrain ceiling jets intensify local heating and promote spread within bays.

4. **Uniformity Hypothesis:** Each structural bay may be treated as a quasi-uniform thermal zone, forming a practical basis for simplified analytical treatments or the use of zone models.

These hypotheses collectively provide a framework for understanding and quantifying the interplay between geometry and fire spread mechanisms. Importantly, they suggest that *fire severity in open car parks is not solely a function of total HRR*, but of how that heat is partitioned spatially within the structure.

The findings lend empirical and theoretical support to the development of simplified zone-based models, in which a car park can be represented as a network of thermally interacting bays. Such models could enable rapid assessment of multiple fire scenarios without the computational expense of full CFD simulations, aiding both performance-based design and regulatory evaluation. The findings of this analysis will be published in the future.

Ongoing research is translating these findings into a parametric zone model capable of estimating fire spread probability and severity in open car parks under varying configurations. Such models could become valuable tools for structural fire engineers, enabling consistent, data-driven evaluation of car park fire resilience without reliance on overly conservative assumptions.

Ultimately, these insights underscore that achieving fire-safe car park design requires an integrated understanding of geometry, fuel load, and environmental conditions—factors that CFD, when carefully calibrated, is uniquely positioned to capture.

References

1. McGrattan, K., Miles, S. (2008). *Modeling Enclosure Fires Using Computational Fluid Dynamics (CFD)*, in *SFPE Handbook of Fire Protection Engineering*, 4th ed.

2. BRE (2010). *Fire Spread in Car Parks.* Crown Copyright, London.

3. Tohir, M. Z. M., Spearpoint, M., Fleischmann, C. (2018). "Prediction of Time to Ignition in Multiple Vehicle Fire Spread Experiments." *Fire and Materials*, 42(1): 69–80.

4. Heskestad, G. (1983). "Luminous Heights of Turbulent Diffusion Flames." *Fire Safety Journal*, 5(2): 103–108.

5. Miechówka, B., Węgrzyński, W. (2025). Systematic Literature Review on Passenger Car Fire Experiments for Car Park Safety Design, Fire Technol. doi:10.1007/s10694-025-01701-5.

6. Deckers, X., Haga, S., Tilley, N., Merci, B. (2013). Smoke Control in Case of Fire in a Large Car Park: CFD simulations of full-scale configurations, Fire Saf. J. 57. doi:10.1016/j.firesaf.2012.02.005.

Fire performance of multi-pane low-energy windows in post-flashover fires

By: Hjalte Bengtsson, Technical University of Denmark, Denmark

The effect of ventilation conditions on the development of compartment fires is a well-described phenomenon, and the impact on the structural response of a building or on the spread of fire to and from façades can be significant. However, most, if not all, fire models such as the Eurocode parametric fire (EN 1991-1-2, annex A) [2] do not consider that new ventilation openings may be created during the fire as window glass breaks and falls out. This is despite fire-induced glass breakage being identified as an important topic of interest for the broad community of fire engineers and fire scientists all the way back in 1985, when Prof. H. W. Emmons presented at the first IAFSS symposium [3]. It is not for the lack of trying, though. Since Prof. Emmon's presentation, several studies have investigated window breakage in fires both in relation to the thermal and mechanical effects on the material level (see an overview in e.g. [4], [5], [6]) and to a lesser extent in relation to the derived effects on the fire (see e.g. [7]).

Most of our knowledge and understanding of the performance of windows in fires relate to legacy windows with single or double layers of glass panes. But modern windows should not be expected to behave like these for several reasons;
  i.   modern windows are typically larger to allow more sunlight into the building,
  ii.   they need toughened glass to withstand the mechanical forces they experience,
  iii. they use low-energy coatings to increase their energy efficiency, and
  iv.   their cavities between panes are filled with argon instead of air to decrease the conductivity and internal convection.
Additionally, at least in the Nordic regions, modern windows have triple layers of glass panes, and often there is a requirement to use laminated safety glass for personal safety. All these factors affect the fire performance in different ways, but the general trend seems to be that the fire resistance of windows has increased over the last 30 years. In relation to windows, fire resistance means both the time until the window cracks and the amount of glass that falls out of the frame, which then forms the actual ventilation opening.

Despite the overall trend and our knowledge of the important impact ventilation conditions have on fire development, our fundamental understanding of glass breakage in modern windows is still limited. Therefore, we decided to look more closely into the subject through a series of tests conducted at the Danish Institute for Fire and Security Technology (DBI).

Figure 1. Picture from one of the tests showing a hot window in the furnace.

Experimental setup

The experimental campaign consisted of eight tests in total. The parameters investigated were the window size (large or small), the number of glass layers (two or three), and the fire exposure (standard fire or parametric fire). An overview of the tests is seen in Table 1.

Table 1. Overview of the different tests.

Specimen ID	Size	Number of glass layers	Fire exposure	Repetition
S-3-B(1)	Small (450 × 450 mm²)	3	Parametric (B)	1
S-3-B(2)				2
L-2-A(1)	Large (1100 mm × 1100 mm²)	2	Standard (A)	-
L-2-B(1)			Parametric (B)	1
L-2-B(2)				2
L-3-A(1)		3	Standard (A)	-
L-3-B(1)			Parametric (B)	1
L-3-B(2)				2

The window sizes were decided by the size of the furnace. The number of glass layers reflected more traditional and more modern types of glazing. The fire curves were chosen to reflect common post-flashover fires with the standard fire curve from EN 1163-1 [8] representing a fierce fast-growing fire, and the parametric fire curve based on a typical residential concrete building with a low opening factor of 0.02 $m^{1/2}$ as described in the Danish National Annex to Eurocode 1 [9] representing a slower and colder fire. The tests did not include the cooling phase of the fire. The temperature-time curves are shown in Figure 4.

All windows were constructed with a wood/aluminium-hybrid frame, and the glazing was made up as follows (described from outside/ambient to inside/fire):

a) Two-layered windows: 4 mm float glass, 16 mm void filled with argon (90 %), 4 mm float glass treated with low-emissivity coating facing the void.

b) Three-layered windows: 4 mm float glass treated with low-emissivity coating facing the void, 18 mm void filled with argon (90 %), 4 mm float glass, 16 mm void filled with argon (90 %), 4 mm float glass treated with low-emissivity coating facing the void.

The windows were fitted in a medium-sized fire test furnace as illustrated in Figure 2. The tests ran for up to 30 minutes, but at least until 5 minutes after cracking of the outermost glass pane. During the tests, the glass temperatures, and in two cases the strains at the edges were recorded. The tests were also filmed which allowed for precise measurement of cracking time and for better estimation of glass fallout areas at different points in time after cracking.
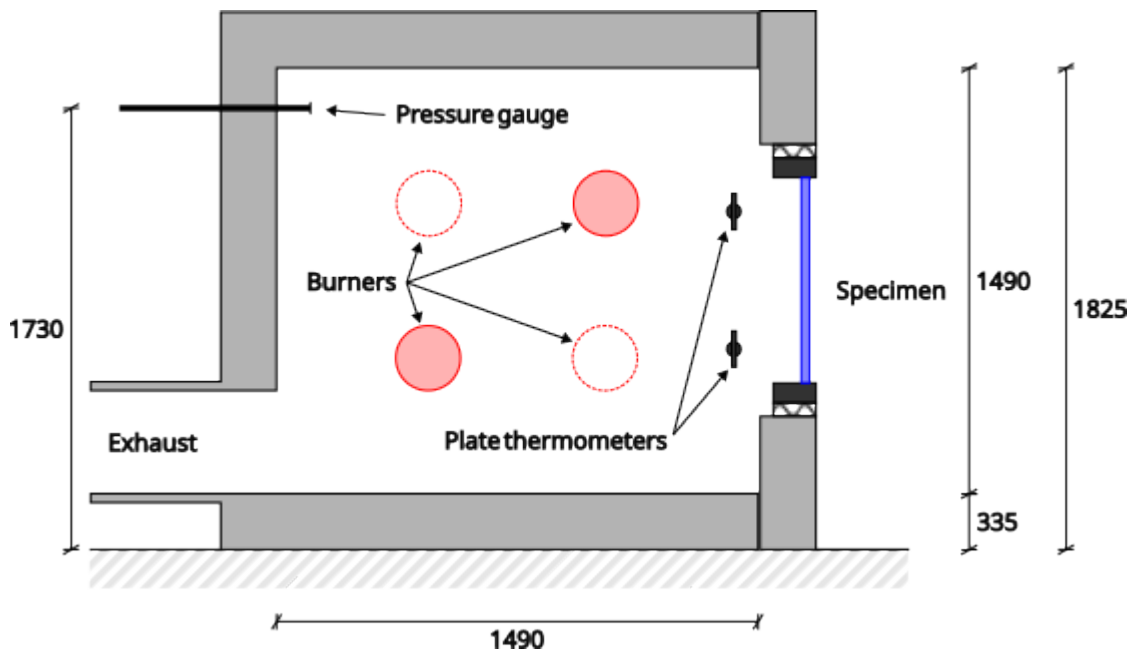

Figure 2. Illustration of the test furnace (vertical cross section) with a mounted specimen. The dashed burners are placed on the opposite wall.

Further descriptions of the experimental setup can be found in the original journal paper [1].

Results

In the following, we will focus on the results for the cracking time and the fallout area. More results and details are presented in the original paper [1].

Cracking time

The results for the cracking time for each of the panes in the glazing in the different tests are seen in Figure 3.
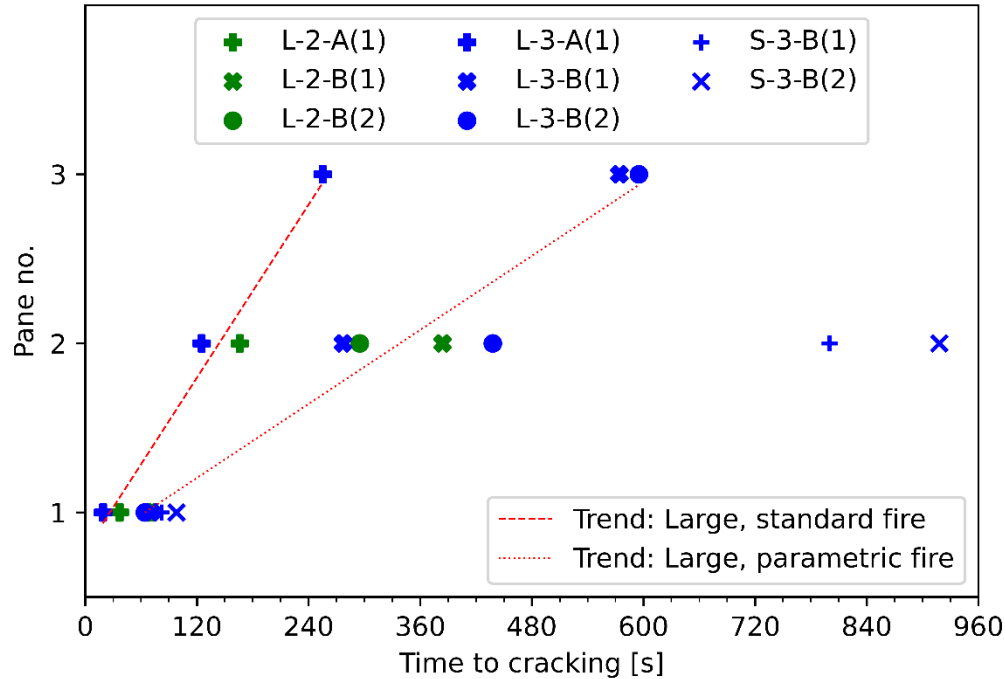
Figure 3. Results for the cracking time for each pane in the tests with different window sizes (S-small or L-Large) different number of panes (2 or 3) and different heating curves (A or B). Note that the third pane in the tests of the small windows (S-3-B(1) and S-3-B(2)) did not crack.

The results show that the panes crack in the order of their placement beginning from the fire side. It is seen that for the parametric fire exposure, the triple layered windows did not have cracking in the outermost until almost 10 minutes after the start of the test, which is almost double the time until cracking of the outmost pane of the double layered windows.

The data suggests that the time between cracking of panes is fixed with the same time between cracking of pane 1 and 2 as between pane 2 and 3. This trend was also seen in the data presented by Peng et al. [10]. This means that the number of panes does not affect the time to cracking of the individual panes. This is seen by the cracking times of the panes following the same linear trend with no regard to the total number of panes. Obviously, having more panes increases the time until all panes have cracked, but the data indicate that the existence of subsequent panes does not impact the cracking time of a given pane.

On the other hand, it is seen that both the window size and the fire intensity have implications for the cracking time. Increasing the fire intensity decreases the cracking times for both the double and triple layered windows. Also, the small windows had a much slower cracking of the second pane compared to the large ones exposed to the same fire curve. Furthermore, the third pane did not crack in the case of the small windows, even though they were exposed to the parametric fire curve for 30 minutes.

We have compared our results of the cracking times for the first (innermost) pane with results for a corresponding calculation in the old software BREAK1 [11] that was developed at Berkeley University in the early 1990's for calculation of cracking times of single pane glazing. We found that the results BREAK1 did not agree with our test results meaning that the software should not be used to predict cracking in modern low-energy windows.

Fallout area

One thing is the cracking time, but the fallout area is ultimately the ventilation opening, and therefore, the single parameter related to window breakage that influences the fire development the most. Figure 4 shows the development in fallout area in time as well as the target furnace temperature of the two

fire curves. The fallout area is measured as the opening area over the total area of the window minus the frame. In the tests, the inner glass panes generally experienced a higher degree of fallout, but that is not reported here as it has little significance in terms of ventilation.
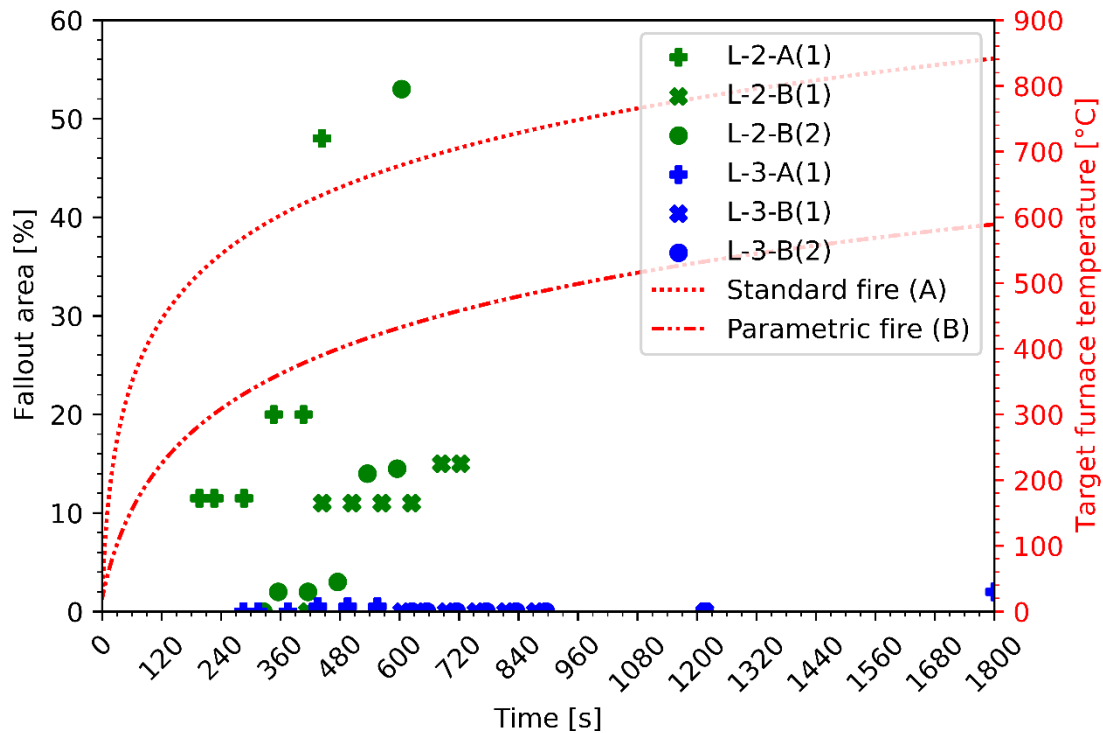

Figure 4. Temperature-time curves or the two fires (right axis) and the fallout area in percentage of the total window area (minus frame area) at different points in time (left axis) for each test.

The most noticeable result in terms of fallout area is the difference between the double, and the triple layered windows. It is seen that the fallout of the triple layered windows was almost 0 % in all three cases (note that the two small windows did not crack and therefore also did not have any fallout, but they are not shown in the figure). In contrast, the final fallout area of the double layered windows was between 15 % and 53 %. This difference between the two groups could lead to vastly different fire developments in a real fire.

The data suggests that the fire intensity has negligible effect on both the initial and the final fallout area as the two parametric fire tests for the double layered windows show vastly different final fallout areas with the standard fire being in between. It is also worth noting that the fallout immediately after cracking is not the final fallout as more glass shards form and fall out of the frame in the time after initial cracking. Initially, the window that ended up with the largest final fallout area had the smallest initial fallout, so initial fallout does not seem to indicate anything about the fallout development. Therefore, only focusing on the cracking time and a set fallout area will not accurately describe the ventilation opening.

Conclusions & future studies

Overall, our experiment shows that the double and triple layered windows result in significantly different ventilation conditions independent of the fire exposure. However, in terms of the mechanisms for cracking times, the two types of windows behave similarly. Additionally, our results show a significant impact of the window size on the fire performance with the small windows ultimately being able to survive the fire without cracking of the outmost pane.

The next steps in our research will be to try to make predictions of the cracking and fallout with simulations in Fire Dynamics Simulator (FDS) to see how well the studied phenomena can be replicated with this fire engineering tool. Additionally, we have planned another series of tests focusing more on the effects of different parameters such as low-emissivity coatings and over-pressure in the fire room. All the publications and activities of the research project are made accessible via our project webpage: https://orbit.dtu.dk/en/projects/low-energy-buildings-and-fire-safety/

References

[1] H. Bengtsson, A. A. A. Awadallah, I. Pope, L. Giuliani, and L. S. Sørensen, "Experimental study of the post-flashover fire performance of multi-pane low-energy windows," *Glass Structures & Engineering*, vol. 10, no. 3, p. 20, Sep. 2025, doi: 10.1007/s40940-025-00305-3.

[2] EN 1991-1-2, *Eurocode 1 - Actions on structures - Part 1-2: Actions on structures exposed to fire*. European Committee for Standardization, 2024.

[3] H. W. Emmons, "The Needed Fire Science," in *Fire Safety Science 1*, C. E. Grant and P. J. Pagni, Eds., International Association for Fire Safety Science (IAFSS), 1986, pp. 33–53. doi: 10.3801/IAFSS.FSS.1-33.

[4] Y. Wang, "The Breakage Behavior of Different Types of Glazing in a Fire," in *The Proceedings of 11th Asia-Oceania Symposium on Fire Science and Technology*, Singapore: Springer Singapore, 2020, pp. 549–560. doi: 10.1007/978-981-32-9139-3_40.

[5] E. Symoens, R. Van Coile, and J. Belis, "Behaviour of Monolithic and Layered Glass Elements Subjected to Elevated Temperatures - State of the Art," in *Challenging Glass 7*, J. Belis, F. Bos, and C. Louter, Eds., Ghent University, Sep. 2020. doi: 10.7480/cgc.7.4489.

[6] H. Bengtsson, L. Giuliani, and L. S. Sørensen, "Fire-induced Glass Breakage in Windows: Review of Knowledge and Planning Ahead," in *8th International Conference on the Applications of Structural Fire Engineering (ASFE)*, Y. Wang and J. Xiao, Eds., Nanning, China: Guangxi University, Feb. 2024, pp. 21–27.

[7] T. Chu, L. Jiang, G. Zhu, and A. Usmani, "Integrating glass breakage models into CFD simulation to investigate realistic compartment fire behaviour," *Journal of Building Engineering*, vol. 82, p. 108314, Apr. 2024, doi: 10.1016/j.jobe.2023.108314.

[8] EN 1363-1, *Fire resistance tests – Part 1: General requirements*. European Committee for Standardization, 2020.

[9] DS/EN 1991-1-2 DK NA, *Nationalt anneks til Eurocode 1: Last på bærende konstruktioner - Del 1-2: Generelle laster - Brandlast*. Denmark: Danish Authority of Social Services and Housing, 2024. [Online]. Available: https://www.bygningsreglementet.dk/nationale-annekser/nationale-annekser/nationale-annekser/

[10] M. Peng, J. Hvidberg, H. Bengtsson, and L. Giuliani, "Fire-Induced Cracking of Modern Window Glazing: An Experimental Study," in *8th International Conference on the Applications of Structural Fire Engineering (ASFE)*, Y. Wang and J. Xiao, Eds., Nanning, China: Guangxi University, Feb. 2024, pp. 201–206.

[11] A. A. Joshi and P. J. Pagni, *Users' Guide to BREAK1, The Berkeley Algorithm for Breaking Window Glass in a Compartment Fire*, NIST-GCR-91-596. National Institute of Standards and Technology (NIST), 1991.

AN OFFICIAL PUBLICATION OF SFPE

SFPE UK Chapter Awards 2025 – Celebrating Excellence and Innovation in Fire Engineering

By: SFPE UK Chapter

Every year, the SFPE UK Chapter Awards shine a light on the individuals and projects pushing the boundaries of fire engineering practice, research, and professional development. Designed to honour excellence across three categories: Fire Engineering Strategy, Fire Research Project, and 'Up & Coming' Fire Engineer. The awards showcase not only technical innovation, but also commitment to community, thought leadership, and the advancement of fire safety knowledge.

The awards underscore a key purpose of the SFPE UK Chapter: to recognise and elevate those who contribute meaningful progress to the fire engineering discipline. Whether through pioneering research, transformative design strategies, or the exceptional promise demonstrated by early-career professionals, the winners embody the values at the heart of the Chapter's mission. In accordance with the official award criteria, the submissions must demonstrate rigour, clarity of purpose, innovative thinking, and tangible benefit to the wider fire engineering community.

The 2025 award cycle saw a record number of submissions from across the UK fire engineering community, reflecting the diversity of challenges facing practitioners today, from emerging materials and technologies to the evolving regulatory landscape shaped by lessons from recent fire incidents. This year's winners represent both depth of expertise and breadth of vision, illustrating how fire engineering continues to evolve through evidence-based practice and collaborative innovation.

We are proud to announce and celebrate the 2025 recipients below.

SFPE UK Chapter Award 2025 – Best Fire Research Project

Winner: Dr Konstantinos Chotzoglou, OFR Consultants, London, UK

Co-author: Michael Spearpoint

Title: Performance Assessment of Fire Spread Between Balconies Using Full-Scale Tests: Bridging the Gap Between Assumptions and Measurements

Recent balcony fires in the UK, including the well-documented incidents at Hallam Court in Croydon (2023) and De Pass Gardens in Barking (2019), have demonstrated the speed with which flames can

spread vertically and laterally between balcony levels. Yet, despite their classification as attachments to the external wall system under Approved Document B, balconies have historically received far less research attention than façades. As highlighted in Dr Chotzoglou's submission, design assumptions have long filled the void left by limited empirical data, a gap the project set out to close through a landmark full-scale testing programme.

The research involved eight full-scale balcony fire experiments, conducted under a 10 MW oxygen-consumption calorimeter, an unprecedented scale for UK balcony fire studies. Each test varied the combination of decking types, balustrade materials (including laminated glass and HPL), and moveable fuel loads to investigate real-world fire behaviour. The bespoke three-storey test rig enabled precise measurement of heat release rate (HRR), heat flux, and fire spread mechanisms across balcony levels.
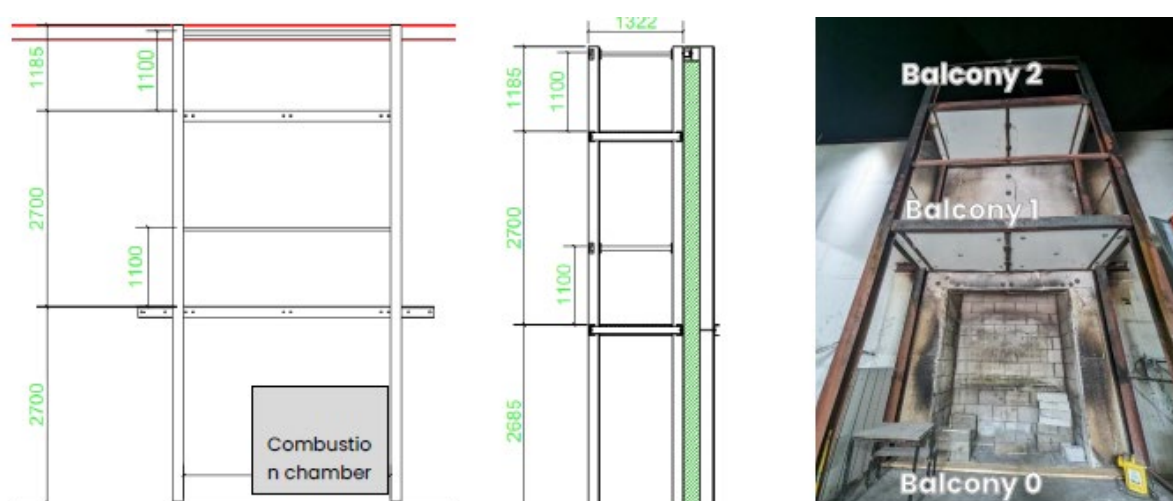

Figure 1. Full-scale balcony test rig constructed under the 10MW calorimeter at Efectis UK/Ireland.

The results were unequivocal: exposed timber decking was the most significant driver of rapid fire growth. Flames reached the balcony two storeys above in 7–9 minutes, with HRR values exceeding 13 MW, in stark contrast to non-combustible decking systems, which exhibited no vertical spread. Laminated glass balustrades provided modest delay but minimal energy contribution, whereas HPL panels markedly intensified fire growth, especially in combination with combustible decking. The incorporation of non-combustible soffits beneath timber decks delayed vertical spread by over 20 minutes and reduced façade heat flux by at least 50%, although they did not fully prevent fire propagation.

The study also introduced significant methodological innovations. Most notably, a qualitative acceptability ranking was developed, providing engineers with a clear hierarchy of fire performance across balcony configurations. In addition, the application of the Fire Growth Rate Index (FIGRA) as a semi-quantitative ranking tool for balcony assemblies for assessing performance in the absence of established test standards.

Table 1. Qualitative ranking of fire spread performance of tests - best to worst. Colours indicate likely acceptability (green - acceptable; orange - marginal; red - unacceptable).

Test ranking	Description
-	Non-combustible deck, non-combustible balustrade, moveable fire load or not
A	Non-combustible deck, open balustrade, no moveable fire load
B	Non-combustible deck, open balustrade, moveable fire load
D	Non-combustible deck, laminated glass balustrade, no moveable fire load
E	Non-combustible deck, laminated glass balustrade, moveable fire load
F	Timber deck with soffit, open balustrade, moveable fire load
-	Timber deck with soffit, laminated glass balustrade, moveable fire load
-	Non-combustible deck, HPL balustrade, moveable fire load or not
H	Timber deck with soffit, HPL balustrade, no moveable fire load
-	Timber deck, laminated glass balustrade, moveable fire load or not
G	Timber deck, HPL balustrade, no moveable fire load
C	Timber deck, open balustrade, moveable fire load

The research has already influenced regulatory and industry discussions, including Building Safety Regulator work relating to Regulation B4(1), and is expected to inform future revisions of BS 8579 and PAS 9980. By replacing assumption with evidence, this work establishes a crucial foundation for safer balcony design and a new benchmark for experimental research in external fire spread.

SFPE UK Chapter Award 2025 – 'Up & Coming' Fire Engineer

Winner: Lorna Johnson, Arup, Edinburgh, UK

Since joining the fire engineering profession in 2022, Lorna Johnson has demonstrated exceptional capability, leadership, and passion, qualities that define the purpose of the "Up & Coming" Fire Engineer Award. Meeting the eligibility criteria as a fire engineering professional with under three years' experience, her submission illustrates not only technical achievement but also strong commitment to knowledge sharing and industry improvement.

Lorna graduated with a First-Class Master's degree in Structural Engineering with Architecture from the University of Edinburgh, where her thesis focused on the fire performance of protective coatings for mass timber. Her experimental research, later presented at the World Conference on Timber Engineering, brought new attention to the limitations of coating systems used in mass timber construction and emphasised the need for deeper understanding as timber becomes more widely adopted.

Figure 2. Presenting at the World Conference on Timber Engineering.

In practice, Lorna has contributed to a variety of challenging and high-profile projects. These include one of Scotland's first large-scale mass-timber developments, where she helped develop a performance-based approach to balance architectural aspirations with fire safety constraints. She played a key role in the fire strategy for the Listed King's Theatre in Edinburgh, undertaking heritage-sensitive risk assessments and supporting on-site evaluations. Her technical involvement in developing Arup's first Building Safety Case submissions under the Building Safety Act 2022 further demonstrates her ability to navigate complex regulatory environments and collaborate across disciplines.

Lorna's drive to advance industry knowledge is evident in her presentations at SFPE conferences, her published work on Building Safety Case lessons learned, and her involvement in Arup's internal advisory group monitoring legislative changes. She has also presented research on EV-related fire risks and submitted further work to upcoming conferences.

Figure 3. 'My Building Safety Case' poster presented at the SFPE Performance Based Design Conference.

Her commitment extends beyond technical work. Lorna actively supports the SFPE Student Chapter in Edinburgh, organising workshops, encouraging early-career engagement, and promoting diversity and inclusion within engineering. Within her team, she is recognised as a source of positivity and cohesion, helping build a collaborative and supportive environment.

Lorna's early career is characterised by curiosity, professionalism, and a genuine desire to contribute to safer and more resilient built environments. Her achievements and attitude reflect both remarkable potential and immediate impact, making her a deserving recipient of the 2025 Up & Coming Fire Engineer Award.

SFPE UK Chapter Award 2025 – Fire Engineering Strategy

Winner: Cameron Milne, Arup, London, UK

Co-authors: Emily Pearson, Judith Schulz, Yavor Panev, Momoi Suda

Project: 50 Fenchurch Street

The winning Fire Engineering Strategy for 2025 recognises the exemplary work undertaken for 50 Fenchurch Street, a 36-storey, all-electric, net-zero-in-operation development set to become one of London's lowest-carbon tall buildings. Designed by Arup for AXA IM Alts and YardNine, the project challenges established high-rise norms and integrates sustainability holistically, including an ambitious external greening scheme extending over 100 metres up two façades and around the top of the tower. This feature alone required a highly innovative fire engineering approach, given its absence from conventional regulatory frameworks.

Figure 4. 50 Fenchurch Street external greening L10 public podium and terrace (@AXA IM Alts).

Sustainability driven design

A key aspect of the strategy was navigating fire safety for the building's extensive external greening, which evolved dramatically during design. Early concepts focused on drought-resistant evergreen species and spatial separation between occupants and planting. However, later design changes introduced amenity balconies and a wider mix of deciduous plants to enhance biodiversity. These shifts required reassessment of ignition risk, moisture content management, and resilience of plant species, under greatly varying microclimates; wind modelling predicted exposure conditions akin to the Cornish coast at upper levels! To demonstrate compliance, the team developed a bespoke large-scale fire test, modifying BS 8414 geometry to represent a credible worst-case balcony-to-greening fire exposure. Conducted at the Fire Protection Association in 2024, the test confirmed that even severe balcony fires would not cause sustained upward fire spread. It also generated valuable empirical evidence on burning brands and flaming droplets for post-test hazard quantification.
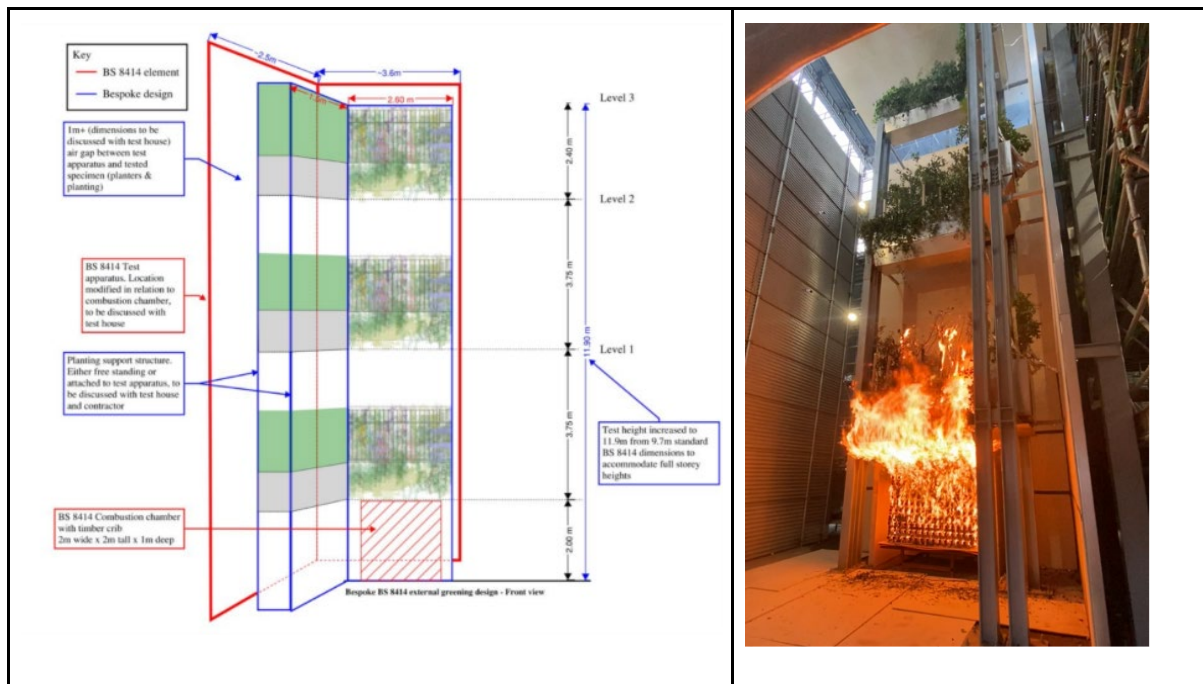
Figure 5. Sketch of the bespoke modified BS 8414 test with large scale fire test.

Equitable means of escape

Beyond greening, the fire strategy addressed next-generation office design through evacuation modelling equitable means of escape, including lift-enabled evacuation. Collaboration with inclusive design specialists and vertical transportation engineers ensured that future diverse user profiles could be safely served, especially in high-occupancy podium levels.

Fire safe structure

Structural fire engineering was another major component. The project's prefabricated "megaplank" system presented limited reinforcement continuity and uncertainties under open-floorplate fire conditions. Through ductile connection detailing, strengthening, LS-DYNA thermomechanical modelling, and a Monte Carlo time-equivalence study, the team optimised fire protection thicknesses while achieving significant reductions in embodied carbon – around 300 tonnes, equivalent to ~300 London–New York flights. Structural robustness analysis investigating multi-storey fire scenarios using advanced FEA was undertaken to maximise flexibility for future tenants.

Addressing novel hazards and other risks

Careful consideration was given to address fire hazards presented by large-scale e-bike charging facilities. Proof-of-concept CFD modelling for all firefighting shafts addressed concerns raised by City of London Building Control.
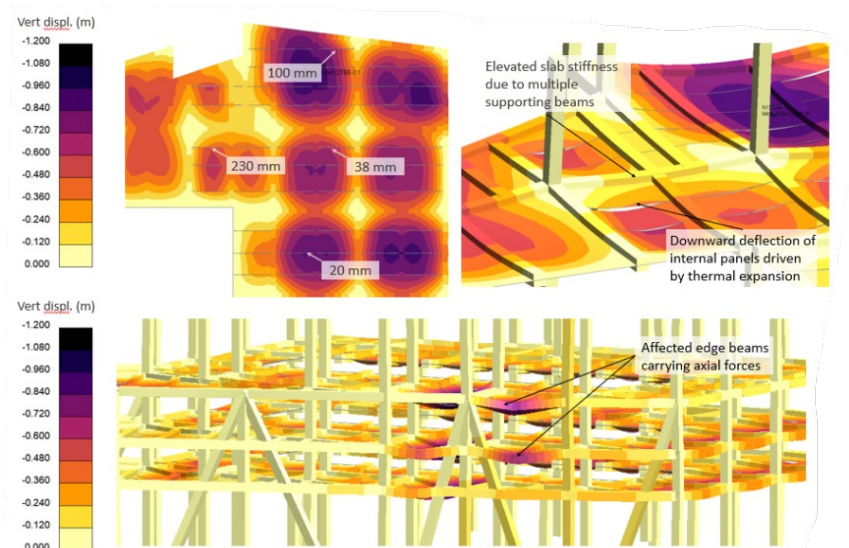
Figure 6. Example challenges of localised differential deflections (top) and reduced lateral restraint (bottom).

Pioneering the future

By maintaining an evidence-led, collaborative, and forward-thinking approach throughout a shifting regulatory environment, the team delivered a robust and future-ready fire strategy that supports both ambitious sustainability goals and exemplary life-safety performance.